

⁶H. Ohnuma, J. R. Erskine, J. P. Schiffer, J. A. Nolen, and N. Williams, *Phys. Rev. C* **1**, 496 (1970).

⁷H. Ohnuma and J. S. Yntema, *Phys. Rev. C* **2**, 1725 (1970)

⁸D. G. Fleming, O. Nathan, H. B. Jensen, and O. Hansen, following paper, *Phys. Rev. C* **5**, 1365 (1972).

⁹J. Bjerregaard, O. Hansen, and G. Sidenius, *Phys. Rev.* **138**, B1097 (1965).

¹⁰J. D. Garrett, R. Middleton, D. J. Pullen, S. A. Andersen, O. Nathan, and Ole Hansen, *Nucl. Phys.* **A164**, 449 (1971).

¹¹R. R. Betts, H. T. Fortune, J. D. Garrett, R. Middleton, D. J. Pullen, and O. Hansen, *Phys. Rev. Letters* **26**, 1121 (1971); T. Caldwell, D. J. Pullen and O. Hansen, *Nucl. Phys.* **A175**, 31 (1971).

¹²T. A. Belote, F. T. Dao, W. E. Dorenbusch, J. Kuperus, and J. Rapaport, *Phys. Letters* **23**, 480 (1966); L. Meyer-Schutzmeister, D. S. Gemmell, R. E. Holland, F. T. Kuchniv, H. Ohnuma, and N. G. Puttaswamy, *Phys. Rev.* **187**, 1210 (1969); A. Graue, J. R. Lien, L. Rasmussen, G. E. Sandvik, and E. R. Cosman, *Nucl. Phys.* **A162**, 593 (1971).

¹³J. H. Bjerregaard, O. Hansen, O. Nathan, R. Chapman, S. Hinds, and R. Middleton, *Nucl. Phys.* **A103**, 33 (1967).

¹⁴R. A. Broglia, C. Riedel, and T. Udagawa, to be published.

¹⁵B. F. Bayman and A. Kallio, *Phys. Rev.* **156**, 1121 (1967); B. F. Bayman, *Phys. Rev. Letters* **25**, 1768 (1970).

¹⁶N. K. Glendenning, *Phys. Rev.* **137B**, 102 (1965).

¹⁷J. R. Erskine, A. Marinov, and J. P. Schiffer, *Phys. Rev.* **142**, 633 (1966); R. Santo, R. Stock, J. Bjerregaard, O. Hansen, O. Nathan, R. Chapman, and S. Hinds, *Nucl. Phys.* **A118**, 409 (1968); J. Yntema, *Phys. Rev.* **186**, 1144 (1969); E. Newman and J. Hiebert, *Nucl. Phys.* **A110**, 366 (1968).

¹⁸E. Kashy, A. Sperduto, H. A. Enge, and W. W. Buechner, *Phys. Rev.* **135B**, 865 (1964); T. W. Conlon, B. F. Bayman, and E. Kashy, *ibid.* **144**, 941 (1966).

¹⁹J. C. Hardy and I. S. Towner, *Phys. Letters* **25B**, 98 (1967); D. G. Fleming, J. C. Hardy, and J. Cerny, *Nucl. Phys.* **A162**, 225 (1971).

²⁰R. J. Petersen, *Phys. Rev.* **170**, 1003 (1968); D. Schmitt and R. Santo, *Z. Physik* **233**, 114 (1970).

²¹E. R. Flynn and O. Hansen, *Phys. Letters* **31B**, 139 (1970).

²²O. Hansen, J. J. Mulligan, and D. J. Pullen, *Nucl. Phys.* **A167**, 1 (1971); R. R. Betts, D. J. Pullen, and O. Hansen, *ibid.* **A182**, 69 (1972).

PHYSICAL REVIEW C

VOLUME 5, NUMBER 4

APRIL 1972

Nuclear Spectroscopy of ^{48}Sc from the $^{46}\text{Ca}(^3\text{He}, p)$ Reaction

Donald G. Fleming,* Ove Nathan, and Hans B. Jensen

The Niels Bohr Institute, University of Copenhagen,† Copenhagen, Denmark

and

Ole Hansen

Los Alamos Scientific Laboratory, University of California,‡ Los Alamos, New Mexico 87544, and Department of Physics, University of Pennsylvania,§ Philadelphia, Pennsylvania 19104

(Received 13 September 1971)

The reaction $^{46}\text{Ca}(^3\text{He}, p)^{48}\text{Sc}$ has been investigated at 18 MeV. Several new spectroscopic assignments have been made for the states in ^{48}Sc up to an excitation energy of 7 MeV. The spectrum is dominated by 1^+ , 2^+ , and 3^+ states. The $1^+ - 7^+$ members of the $(f_{7/2})^{-1}f_{7/2}$ multiplet are very weakly populated and this result is consistent with distorted-wave Born-approximation calculations based on such a model. The presence of configuration mixing in the low-spin members of the multiplet is deduced from a distorted-wave analysis of the cross sections; in particular the 6.685-MeV $0^+ T=4$ state (the analog of the ^{48}Ca ground state) was found to be populated about 5 times stronger than predicted by the simple $(f_{7/2})^{-1}f_{7/2}$ model. This enhancement factor is similar to the one found in the reaction $^{46}\text{Ca}(t, p)^{48}\text{Ca}(\text{g.s.})$ and can be explained in terms of small admixtures of $2s-1d$ hole components in the ^{46}Ca ground state and of $2p-1f$ configurations in the ^{48}Ca ground-state wave functions.

I. INTRODUCTION

The nucleus ^{48}Sc is important from the shell-model point of view, since the lowest-lying levels can be thought of in terms of the coupling of an $f_{7/2}$ neutron hole and an $f_{7/2}$ proton particle outside of a closed ^{46}Ca core. This configuration gives

rise to eight positive-parity states with spins ranging from 0 to 7 and such states now appear to be experimentally well established from $(^3\text{He}, t)$ and nucleon-pickup reactions.¹⁻⁴ In addition to the levels of the $(f_{7/2})^{-1}f_{7/2}$ multiplet, the pickup reactions provide information on the $2s-1d$ hole states in ^{48}Sc .

With the exception of states in the $(f_{7/2})^{-1}f_{7/2}$ multiplet and a recent report on 1^+ states,⁵ little information exists on the higher-lying states in ^{48}Sc . In this respect the $(^3\text{He}, p)$ reaction is well suited, since particle configurations which lie beyond the $f_{7/2}$ shell may be strongly populated. It is the purpose of this paper to report on spectroscopic assignments for the levels excited in the reaction $^{46}\text{Ca}(^3\text{He}, p)^{48}\text{Sc}$ up to 7 MeV of excitation energy. These transitions are expected to be composed primarily of configurations which can be constructed from the $1f-2p$ shell and thus to populate states of positive parity.

II. EXPERIMENTAL RESULTS AND EMPIRICAL SPIN ASSIGNMENTS

A. Procedures and Results

The experiment was carried out with the 18-MeV ^3He beam from the University of Pennsylvania tandem accelerator. The target was isotopically pure ^{46}Ca produced by mass-separator implantation in a carbon foil of about $40 \mu\text{g}/\text{cm}^2$ thickness, as described elsewhere.⁶ The target was quite inhomogeneous and its effective thickness was unknown, so that absolute cross sections could not be obtained. The $(^3\text{He}, p)$ angular distributions were measured with a multigap magnetic spectrograph in an angular range from 3.8 to 87.8° in steps of 7.5° . The energy resolution was typically 35 keV full width at half maximum. A spectrum measured in the first gap is displayed in Fig. 1, and the experimental data and empirical spin assignments are given in Table I.

The ground state was weakly excited and its position on the photographic plates could not be determined accurately. Consequently the excitation energies were determined relative to the strongly excited 6.685-MeV $T=4$ state in ^{48}Sc ,⁷ except for the lowest five excited states, where the more accurate (± 10 keV) values of Ohnuma *et al.*² were used. The table also lists the summed cross sections in the first 10 gaps and the observed maximum cross section.

B. Empirical Systematics of the Angular Distributions

The observed angular distributions are displayed in Figs. 2-5, grouped according to spin assignments, as discussed below. The spin and parity assignments for many of the low-lying states in the neighboring nucleus ^{50}Sc ($J=1^+-5^+$) now seem well established,⁸⁻¹⁰ and we have used the observed shapes of the $(^3\text{He}, p)$ angular distributions for these states¹¹ as a guide in the interpretation of the distributions in ^{48}Sc . The ^{50}Sc angular-distribution data at 18-MeV bombarding energy for

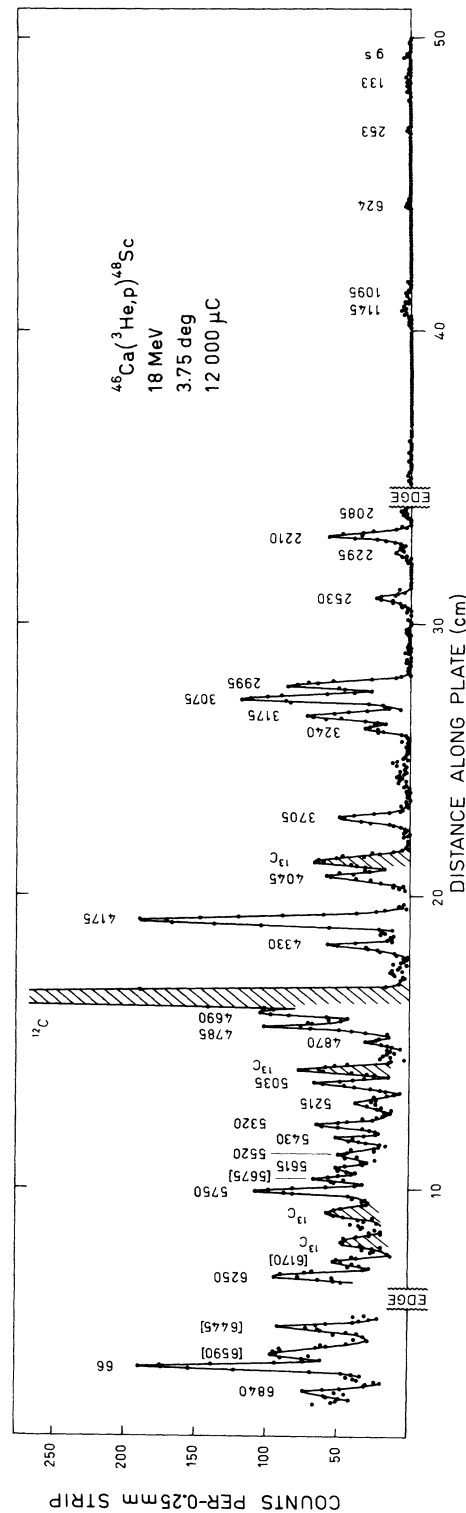


FIG. 1. Energy spectrum for the reaction $^{46}\text{Ca}(^3\text{He}, p)^{48}\text{Sc}$ at 3.75 MeV. The resolution is 35 keV. The peaks given with a cross-hatch are impurity lines. Those few excitation energies given in square brackets are peaks for which angular distributions were not obtainable. Note the very weak population of the low-lying states of the $(f_{7/2})^{-1}f_{7/2}$ multiplet.

the low-lying $1^+ - 5^+$ states are displayed in Fig. 6. The curves in Fig. 6 serve to guide the eye and are not optimized to give the best account of these particular transitions. Rather they have been chosen to give a representation of many such distribu-

TABLE I. $^{46}\text{Ca}(^3\text{He}, p)^{48}\text{Sc}$ excitation energies, assignments, and cross sections.

E_x (keV) ^a	J_f ^b	$\sum \sigma$ ^c (arb. units)	σ_{max} ^d (arb. units)
0	6	100 ± 50	20
133	5	150 ± 50	20
253	4	150 ± 50	30
624	3	300 ± 100	70
1095	7	300 ± 150	40
1145	2	550 ± 100	140
2085 ± 15	4, 5	1200 ± 200	200
2210 ± 15	2, 3	4300 ± 500	950
2295 ± 15	2, 3	2000 ± 300	450
2530 ± 15	1	500 ± 100	250
2690 ± 20	4, 5	500 ± 100	130
2995 ± 15	1	2500 ± 300	1080
3075 ± 15	1	3700 ± 400	1650
3175 ± 15	1	2100 ± 300	950
3240 ± 20	1, 0	800 ± 200	300
3510 ± 20	2, 3	550 ± 150	130
3705 ± 15	1	2000 ± 300	600
4045 ± 20	1	1700 ± 200	600
4175 ± 15	1	6900 ± 800	2700
4330 ± 20	1, 0	1700 ± 300	550
4690 ± 15	1	2900 ± 400	850
4785 ± 15	1	3300 ± 500	1000
4870 ± 15	2, 3	2000 ± 300	400
5035 ± 20	2, 3	1600 ± 400	300
5215 ± 15	2, 3	2100 ± 400	500
5350 ± 15	2, 3	3000 ± 500	800
5430 ± 25	1	850 ± 250	350
5520 ± 20	2, 3	1500 ± 500	450
5615 ± 20	2, 3	1700 ± 500	450
5750 ± 15	1	3000 ± 500	900
6250 ± 15	2, 3	3800 ± 600	800
6685 ($T=4$)	0	5200 ± 800	2100
6840 ± 20	1, 2, 3	2000 ± 600	500
6955 ± 15	1, 2, 3	4000 ± 800	900

^a Excitation energies of first five excited states are taken from the $(^3\text{He}, t)$ results of Ref. 2. The remaining energies are given relative to the 6685-keV state (Ref. 7).

^b All levels are assumed to be of positive parity, as discussed in the text.

^c Summed cross sections (not weighted by $\sin\theta$) from 3.9 to 73.0° c.m. Beyond 5-MeV excitation energy, ^{15}N groups from the ^{13}C in the target backing obscured some ^{48}Sc states at particular angles. In these cases, the smooth curves of Fig. 6 were used to define the cross sections.

^d The maximum observed cross section.

tions of closely similar shapes in both ^{48}Sc and ^{50}Sc . As such, they are referred to as "average curves." Although one cannot justify the concept of such average curves from simple theoretical arguments (in particular not for the odd-spin states which may be excited by transitions of mixed L value), we have found their use to be helpful for an empirical classification of the observed distributions. In this way we arrive at three main classes of states: 1^+ states (Fig. 2); (1^+), 2^+ , and 3^+ states (Figs. 3 and 4); and higher-spin states (Fig. 5).

The 1^+ distributions of Fig. 2 are dominated by a sharp decrease with increasing angle in the range from 4 to 20°. The average 1^+ curve, with its 25° "plateau," is distinctly different from the curve shown for the 6.685-MeV, 0^+ , $T=4$ state in the same figure. This distinction between 0^+ and 1^+ , as well as the spectrum of 1^+ states in ^{48}Sc , is discussed in detail in Ref. 5.

Figures 3 and 4 display the distributions that are similar to those obtained for transitions to known 2^+ and 3^+ states (Fig. 6). As such, they are thought to correspond primarily to an $L=2$ transfer. The shapes in Fig. 3 exhibit a strong decrease towards 0° , whereas the Fig. 4 shapes are flat near 0° . This effect cannot be associated with the final-state spin, since, for example, the distribution for the 624-keV 3^+ state (Fig. 3) and the distribution for the 255-keV 2^+ level in ^{50}Sc (Fig. 6) show the same decrease towards 0° . The causes for the existence of the two different shapes for 2^+ , 3^+ excitations are not understood. It is unlikely that much of this effect is due to an $L=4$ component in the 3^+ transitions (cf. Figs. 5, 6).

It should also be stressed that an unambiguous $J^\pi = 2^+, 3^+$ assignment cannot be made to the final states of Figs. 3 and 4, because $J^\pi = 1^+$ cannot be rigorously excluded. According to the selection rules for direct $(^3\text{He}, p)$ reactions, 1^+ final states can be reached from 0^+ targets by $L=2$ transitions. Inside the configuration space of interest, however, only one 1^+ configuration, $2p_{3/2}1f_{5/2}$, would not carry a detectable $L=0$ component.

Figure 5 displays the distributions corresponding to states of spin higher than 3 observed in the $^{46}\text{Ca}(^3\text{He}, p)$ reaction. Only four such states could be identified in the data, reflecting the fact that the $(^3\text{He}, p)$ reaction preferentially excites states of lower spin. Unlike the $2^+, 3^+$ states, there appears to be a shift of about 10° in the maximum of the angular distribution between states of spin 4^+ and 5^+ . This shift is evident in the ^{50}Sc data of Fig. 6 and also in the data of Fig. 5. However, we do not attempt to distinguish between 4^+ and 5^+ on this basis and prefer to classify these states as ($4^+, 5^+$). It should be noted that while $J^\pi = 3^+$

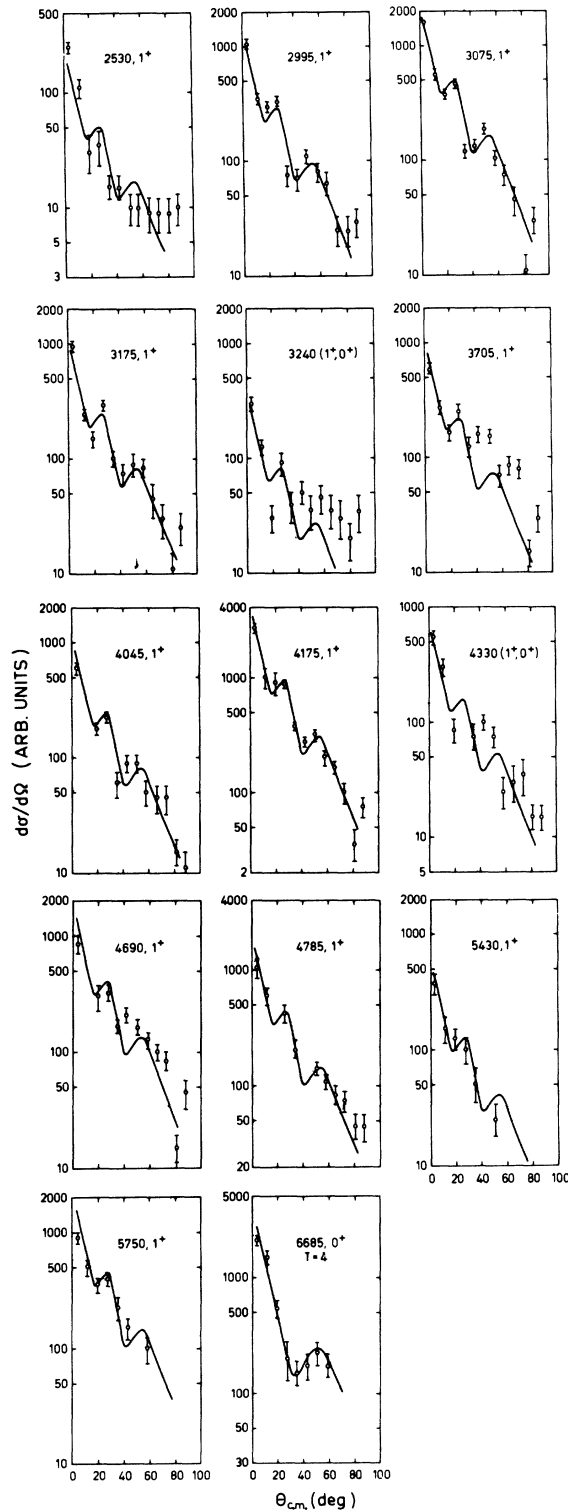


FIG. 2. The 1^+ states assigned in ^{48}Sc . The same 1^+ curve (taken from Fig. 6) is drawn through all transitions and can only be expected to reproduce the forward-angle behavior of the data. The 6685-keV $T=4$ transition is pure $L=0$ and this is represented by a different curve.

cannot be rigorously excluded from this category of transitions, such a final spin is unlikely; the lowest 3^+ configurations giving rise to pure $L=4$ transitions are $s_{1/2}g_{7/2}$ and $p_{3/2}h_{9/2}$, both outside the configuration space of importance here.

III. DISTORTED-WAVE BORN-APPROXIMATION ANALYSIS AND NUCLEAR-STRUCTURE CALCULATIONS

A. States in the $(f_{7/2})^{-1}f_{7/2}$ Multiplet

As noted above, the level positions of the states in the $(f_{7/2})^{-1}f_{7/2}$ multiplet now seem well established.¹⁻⁴ These multiplet states should also be observable in the reaction $^{46}\text{Ca}(^3\text{He}, p)^{48}\text{Sc}$ because of the predominant $(f_{7/2})^{-2}$ hole structure of the ^{46}Ca ground state. The spectroscopic overlaps for these states in the $(^3\text{He}, p)$ reaction are the same for every state in the multiplet, independent of J , under the assumption of a pure $(f_{7/2})^2$ transfer configuration. However, with the exception of the 6.685-MeV, 0^+ , $T=4$ state, they are all observed to be only weakly excited. Indeed, the summed cross sections (Table I) of the 1^+-7^+ states of the $(f_{7/2})^{-1}f_{7/2}$ configuration represent less than 5% of the total. This result is in contrast to the $^{48}\text{Ca}(^3\text{He}, t)^{48}\text{Sc}$ data,^{1,2} where the $(f_{7/2})^{-1}f_{7/2}$ states are among the strongest.

The distorted-wave Born-approximation (DWBA) calculations were carried out with the zero-range code DWUCK (developed by P. D. Kunz, University of Colorado), employing both a Woods-Saxon¹² (WS) and harmonic-oscillator¹³ (HO) form factor for the transferred neutron-proton pair. The calculated angular-distribution shapes were practically independent of the choice of code. Several optical-model combinations from different parameter sets appearing in the literature^{9, 14-17} were tried in the $(^3\text{He}, p)$ analysis. Some representative choices made are given in Tables II and III. The parameters given in these tables are quoted as they are entered in the DWUCK code. The coding is such that both the derivative form of the imaginary potential and the strength of the spin-orbit potential are 4 times larger than the original Perey definition.^{16, 17}

The distorted-wave (DW) fits utilizing the A and X optical-model potentials of Tables II and III, respectively, for most of the states of the multiplet are given in Fig. 7. The ground-state (6^+) and 133-keV (5^+) transitions were very weakly excited (Fig. 1) and the angular-distribution data were of poor quality, so DW fits to these data are not given. The calculated curves are individually normalized in Fig. 7. The AX potential gave the best fit to the data for the $(f_{7/2})^{-1}f_{7/2}$ transitions, although the results of the CZ potential were rather

similar. It is the AX combination, without the spin-orbit term, which also gave satisfactory fits to the 18-MeV $^{48}\text{Ca}(^3\text{He}, p)^{50}\text{Sc}$ data of Schlegel *et al.*⁹ We find that the inclusion of the spin-orbit force makes some difference on the calculated shapes at forward angles, but little change in the relative cross sections discussed below. The BY potentials consistently gave the poorest fits to the $(f_{7/2})^{-1}f_{7/2}$ data. Note that a satisfactory account of the shapes of the 624-keV 3^+ and 1145-keV 2^+ transitions is obtained with the AX potential. Both of these transitions show the forward-angle $L=2$ dip referred to earlier. The 1^+ DW fit appears not to have enough $L=2$ component, but the calculated shapes of the other transitions are in good agreement with the data using this potential combination.

The calculated cross sections obtained with the HO code are compared with the observed cross sections for the $(f_{7/2})^{-1}f_{7/2}$ transitions in Table IV. The three optical-model combinations AX, BY, and CZ have been used in the DW calculations. All cross sections are given relative to that of the 624-keV 3^+ state. A normalization to any of the higher-spin states would be unreasonable with the present data because of the low accuracy obtained in the corresponding cross sections (Table I).

In the $(^3\text{He}, p)$ reaction there is a strong spin dependence^{18, 19} expected which favors the $S=0$

transfer over the $S=1$ by a factor of about 3, although the calculation of this factor from experimental data depends somewhat on the method used to construct the two-nucleon form factor.²⁰ In accordance with Ref. 19, we have used an enhancement factor of 3 for the $(f_{7/2})^{-1}f_{7/2}$ multiplet states of even spin in Table IV, since these can only be populated by pure $S=0, T=1$ transfers.

The over-all agreement concerning relative cross sections between the $f_{7/2}$ theory and the data for the multiplet states is not satisfactory. The discrepancies which appear from Table IV clearly are connected with the spin values: With the normalization chosen the relative strength of the 0^+ state is 4–5 times higher than predicted, whereas the relative strength of the high-spin states is 2–3 times lower than predicted. Over the full range of spin values the pure $f_{7/2}$ theory thus gives rise to a discrepancy in the cross section by more than a factor of 10.

Since the comparison between the two form-factor procedures is of interest, the theoretical $(f_{7/2})^{-1}f_{7/2}$ cross sections obtained with the WS form factor are also given in Table IV. The binding energy of each nucleon was taken to be $\frac{1}{2}$ the separation energy of the pair. Note that the HO results and the WS results are similar, in particular the large discrepancy in the analog-state transition is unchanged.

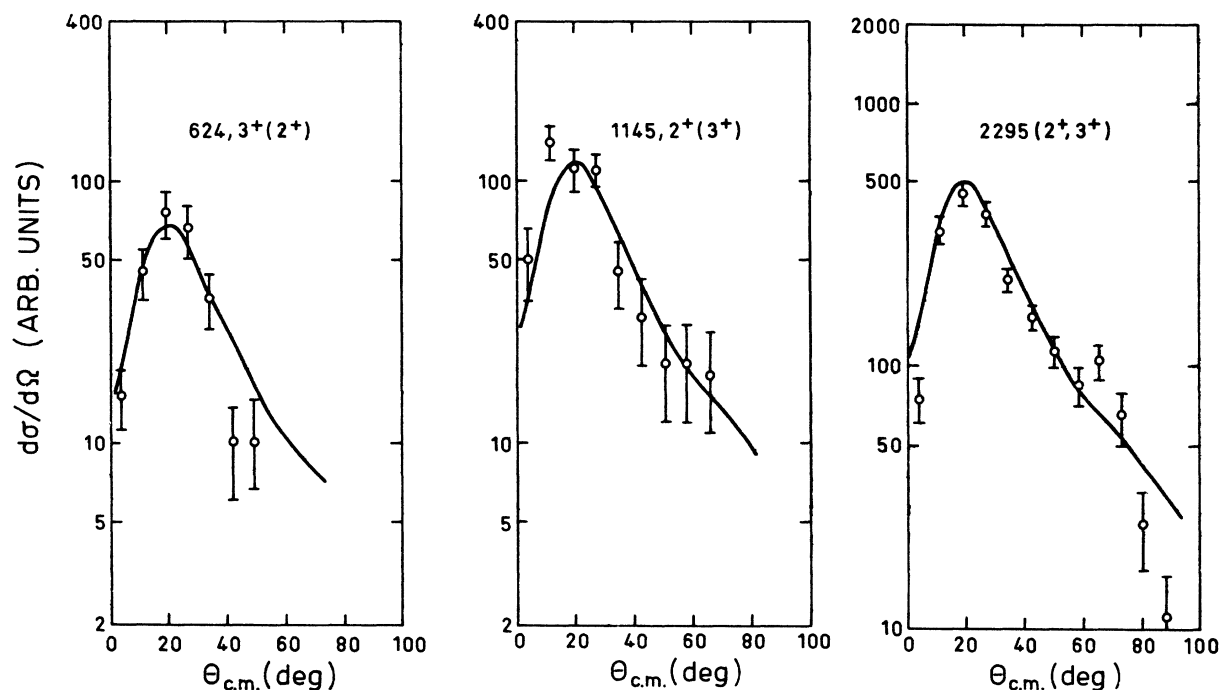


FIG. 3. Some $(2^+, 3^+)$ $L=2$ transitions in ^{48}Sc which show a pronounced forward-angle dip in the cross section. The curves drawn through the data are only meant to guide the eye but it is the same curve for all transitions and it is taken from Fig. 6.

B. Higher-Lying States and Comparison
with the Reaction $^{46}\text{Ca}(^3\text{He}, t)^{48}\text{Sc}$

As can be seen in Table I and in Fig. 1, the majority of the experimental strength found in the reaction $^{46}\text{Ca}(^3\text{He}, p)^{48}\text{Sc}$ occurs beyond 2 MeV. Since, to our knowledge, wave functions other than pure $(f_{7/2})^{-1}f_{7/2}$ are not available for ^{48}Sc , we are unable to make any quantitative comparison of the states beyond 2 MeV with a realistic nucle-

ar model. However, the effects of a more expanded model space may be examined in rough outline. The higher configurations of the $2p$ shell will carry much more cross section in the two-nucleon-transfer reaction than those of the $f_{7/2}$ shell. This point has recently been emphasized by Bayman²¹ and is also borne out in the discussion to follow.

In Table V we present cross sections calculated with the HO form factor using pure configurations other than $(f_{7/2})^{-1}f_{7/2}$ for selected higher-lying states in ^{48}Sc . The cross sections are given (in the same units) relative to the theoretical $(f_{7/2})^{-1}f_{7/2}$ 3^+ cross section of Table IV. They are given only for the AX optical model, since the results of other potentials were very similar, as can be seen already from Table IV. The theoretical $(^3\text{He}, p)$ cross sections of Table V were calculated assuming $(f_{7/2})^{-1}f_{5/2}$, $(f_{7/2})^{-1}p_{3/2}$, $(p_{3/2})^2$, and $p_{1/2}p_{3/2}$ configurations. In addition, the

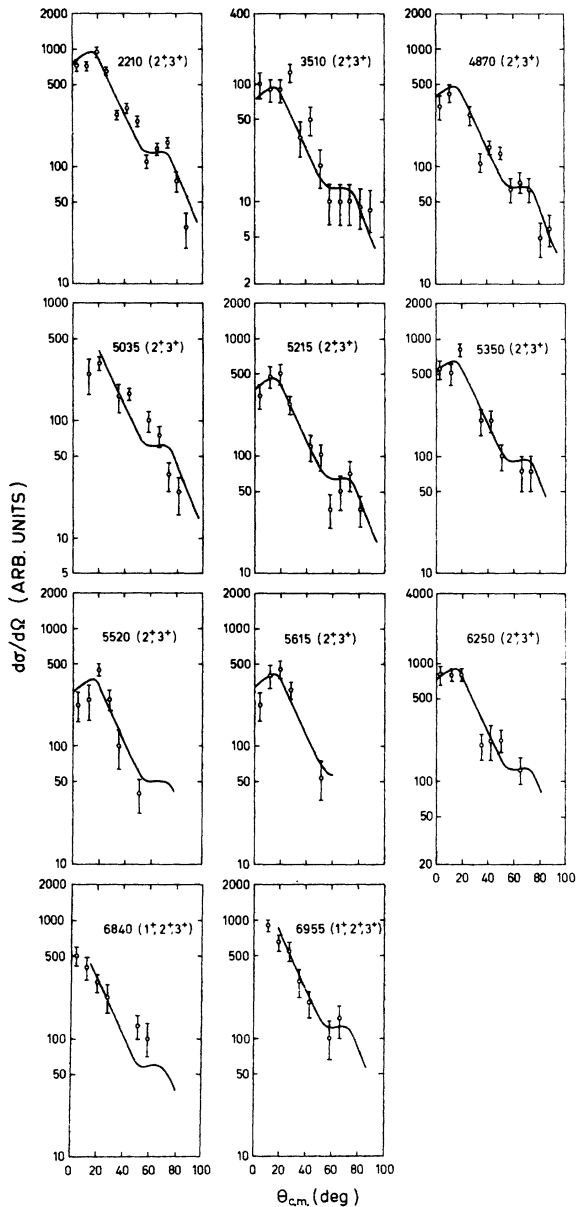


FIG. 4. The $(2^+, 3^+)$ $L=2$ transitions in ^{48}Sc which show a flattened shape at the forward angles. See caption to Fig. 3. A possible 1^+ assignment cannot be excluded for the 6840- and 6955-keV transitions.

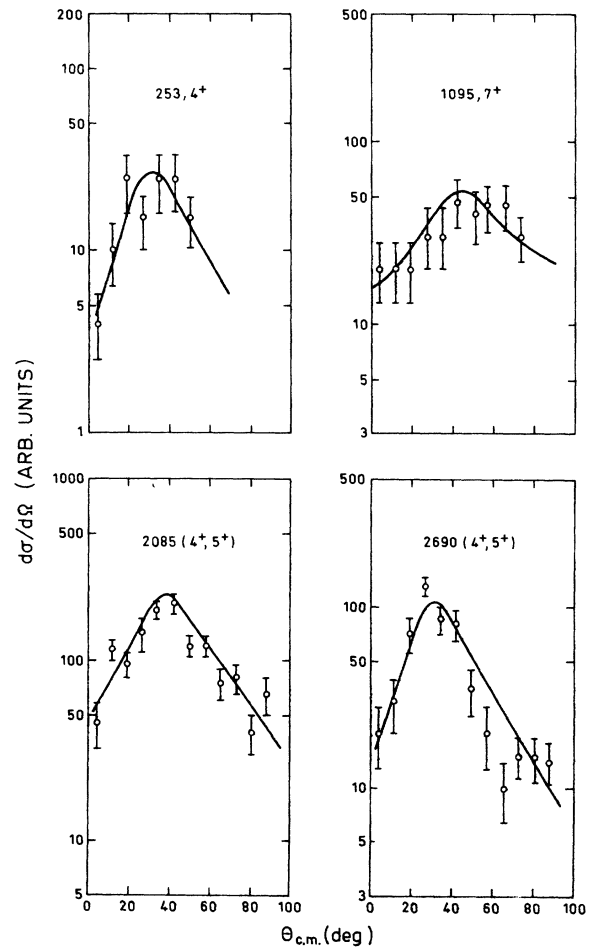


FIG. 5. Transitions to states of higher spin populated in the $^{46}\text{Ca}(^3\text{He}, p)$ reaction. The curves are drawn to guide the eye and, with the exception of the 1095-keV 7^+ transition, are taken from Fig. 6.

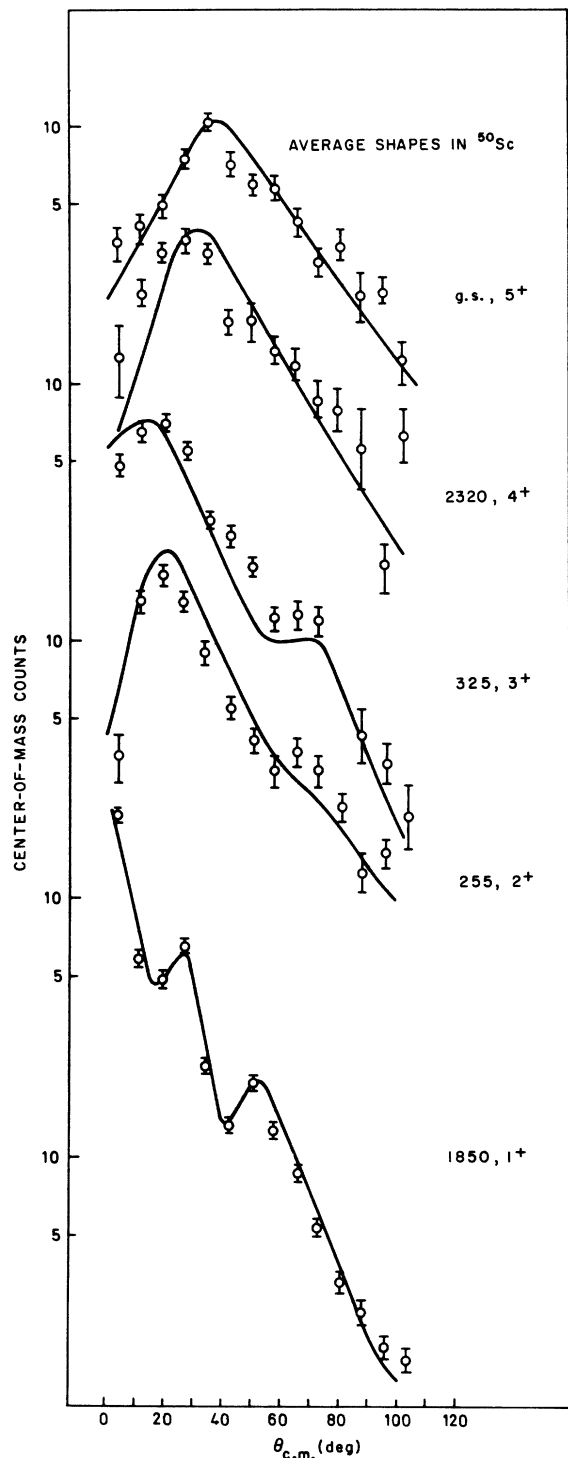


FIG. 6. Angular distributions for states of known spin ($1^+ - 5^+$) observed in the reaction $^{48}\text{Ca}(^3\text{He}, p)^{50}\text{Sc}$ (Ref. 11) at 18-MeV bombarding energy. The curves are only to guide the eye and are meant to give a reasonable account of all such transitions of similar shape observed in both ^{46}Ca and $^{48}\text{Ca}(^3\text{He}, p)$ reactions. The ordinate does not give the relative cross sections.

$(f_{7/2})^{-1}f_{7/2}$ calculations of Table IV are repeated for the higher excitation energies, in order to examine the Q dependence of the calculated cross sections. As can be seen from Table V, this is most important for the $L=2$ transitions, although even in this case the effect of a 4-MeV decrease in the Q value makes only about a 35% increase in the calculated cross sections. The Q dependence of the $(^3\text{He}, p)$ cross sections in this mass region is then generally weak, a point which has also been discussed with regard to the 1^+ states in Ref. 5.

The cross sections predicted for $2p$ shell form factors are much larger than those calculated for the $(f_{7/2})^{-1}f_{7/2}$ configuration. Certainly the pure configurations given in Table V cannot be construed as giving any accurate representation of the actual wave functions for the states chosen and, indeed, good fits to the angular-distribution data for the higher-lying states were not achieved. However, the calculations given in Table V do show that the bulk of the cross section in the reaction $^{46}\text{Ca}(^3\text{He}, p)^{48}\text{Sc}$ will come from the orbits of the $2p$ shell and are thus in qualitative agreement with the weak population of the $1^+ - 7^+$ members of the $(f_{7/2})^{-1}f_{7/2}$ multiplet (Table I, Fig. 1).

The $(^3\text{He}, p)$ transitions to the states at 3075,

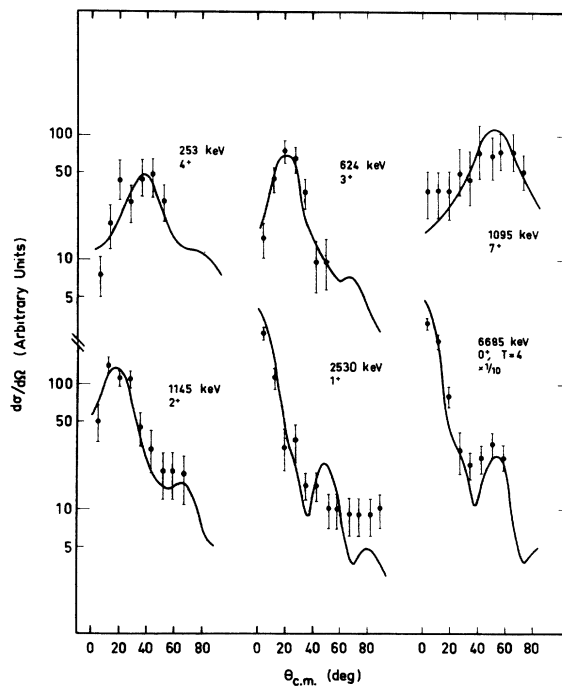


FIG. 7. DWBA fits to the states of the $(f_{7/2})^{-1}f_{7/2}$ multiplet observed in the reaction $^{46}\text{Ca}(^3\text{He}, p)^{48}\text{Sc}$. Each curve is individually and arbitrarily normalized to the data. The optical potential used is the AX combination of Tables II and III.

TABLE II. ${}^3\text{He}$ optical-model parameters.

Label	V	r_V	a_V	W	r_W	a_W	V_{so}	r_{so}	a_{so}	r_C	Reference
A	165	1.14	0.72	20.2	1.60	0.81	28.0	1.14	0.72	1.15	9 ^a
B	157	1.24	0.66	16.0	1.59	0.86	0.0			1.15	14 ^b
C	182	1.15	0.71	15.1	1.64	0.79	0.0			1.15	15 ^c

^a ${}^3\text{He}$ parameters from the 18-MeV ${}^{48}\text{Ca}({}^3\text{He}, p){}^{50}\text{Sc}$ DW analysis but including a spin-orbit term.

^b Taken from 20-MeV triton scattering on ${}^{40}\text{Ca}$.

^c 18.8-MeV ${}^3\text{He}$ scattering on ${}^{40}\text{Ca}$.

3175, 3240, 3510, and 3705 keV agree in excitation energy, within the experimental errors, with states at 3068, 3179, 3230, 3495, and 3690 keV observed in the $({}^3\text{He}, t)$ reaction.² Possibly the 4330-keV level from the present experiment may correspond with the 4265-keV 1^+ state reported in Ref. 2. Other than these states, only the members of the $(f_{7/2})^{-1}f_{7/2}$ multiplet are common in the two reactions. Our 3075-, 3175-, 3240-, and 3705-keV levels are all assigned 1^+ or $1^+, 0^+$, but these assignments are difficult to reconcile with the $({}^3\text{He}, t)$ angular distributions for the 3179- and 3690-keV states as presented in Ref. 2; the $({}^3\text{He}, t)$ data perhaps indicate higher-spin values (see also Ref. 1). In view of the high level density of ${}^{48}\text{Sc}$ at these excitation energies²² it may not be meaningful, however, to compare the two sets of reaction data. The excitation of so many 1^+ states in this energy region in the $({}^3\text{He}, t)$ reaction would be difficult to understand on the basis of a closed ${}^{48}\text{Ca } f_{7/2}$ neutron shell.

C. Odd- L Transfers in the $({}^3\text{He}, p)$ Reaction

In Fig. 8 we compare the calculated DW shapes for transitions of negative parity, $L=1, 3,$ and 5 with those of positive parity $L=0, 2, 4,$ and 6 . The DW curves of Fig. 8 are for an excitation energy of 3.4 MeV in ${}^{48}\text{Sc}$ and are calculated with the AX optical potential. Only pure L transfers are shown. The transitions of positive parity (solid lines) are calculated assuming an $(f_{7/2})^{-1}f_{5/2}$ configuration, while those of negative parity (dashed lines) were obtained assuming an $(f_{7/2})^{-1}g_{9/2}$ configuration. Only the $L=0$ and $L=1$ transfers are

forward peaked, with the latter showing a flatter behavior in this angular region. It is clear from Fig. 8 that the shapes of $L=0$ and $L=1$ transitions are both very distinct from those of higher L values. Unfortunately, the large majority of observed $({}^3\text{He}, p)$ transitions have mixed L values and thus do not correspond to any of the curves of Fig. 8. In fact, most of the observed $({}^3\text{He}, p)$ shapes can be reproduced reasonably well by more than one arbitrary combination of L values and we conclude that the parity of the final state cannot be determined on the basis of calculated shapes alone.

However, for the states of low spin, we find that a comparison of empirical shapes often allows a fairly reliable determination of the final parity. This is particularly true for the 1^+ states. Other than $L=0$, only $L=1$ transitions show a rise in forward angles (Fig. 8), but the available data indicate that $({}^3\text{He}, p)$ transitions dominated by $L=1$ show a much flatter shape at forward angles²³ than we observe for the 1^+ transitions (Fig. 2). Consequently, 1^+ should be safely distinguished from 1^- and 2^- final states. Similarly $L=3$ transitions are not observed to be forward peaked.²³ The preponderance of positive-parity states that we assign in ${}^{48}\text{Sc}$ below 6 MeV (Table I) is also consistent with the very weak spectroscopic strengths measured^{24, 25} to the $2s-1d$ hole states in ${}^{46}\text{Ca}$ and ${}^{48}\text{Ca}$.

D. 6.685-MeV $0^+ T=4$ Transition

It appears from Table IV that the pure $(f_{7/2})^{-1}f_{7/2}$ model is quite inadequate to account for the experimental relative cross section to the 6.685-MeV analog state in the reaction ${}^{46}\text{Ca}({}^3\text{He}, p){}^{48}\text{Sc}$. Even

TABLE III. Proton optical-model parameters.

Label	V	r_V	a_V	W_D	r_D	a_D	V_{so}	r_{so}	a_{so}	r_C	Reference
X	52.5	1.21	0.75	56.5	1.20	0.47	32.0	1.21	0.75	1.20	9 ^a
Y	49.7	1.24	0.69	48.8	1.28	0.46	35.2	1.24	0.69	1.20	16 ^b
Z	50.0	1.20	0.75	48.0	1.20	0.70	0.0			1.20	c

^a Proton parameters from 18-MeV ${}^{48}\text{Ca}({}^3\text{He}, p){}^{50}\text{Sc}$ DW analysis.

^b Perey potential for 17-MeV protons on Fe but with the real well taken from the "best-fit" potential of Bechetti and Greenlees (Ref. 17).

^c Essentially same as Y potential but containing no spin-orbit term.

TABLE IV. Relative cross sections for the states of the $(f_{7/2})^{-1}f_{7/2}$ multiplet.

E_x (keV)	J	$\sum \sigma(\text{exp})^a$	$\sum \sigma(\text{HO})^b$			$\sum \sigma(\text{WS})^b$
			AX	BY	CZ	AX
0	6^+	35	120	75	135	125
133	5^+	50	110	120	115	120
253	4^+	50	165	135	135	160
624	3^+	100	100	100	100	100
1095	7^+	100	215	190	340	275
1145	2^+	185	245	195	225	220
2526	1^+	165	185	150	170	145
6685	0^+	1750	420	380	450	300

^a The experimental cross sections are relative to a value of 100 for the 624-keV 3^+ transition and are taken from the summed cross sections of Table I.

^b The theoretical cross sections are labeled by the optical-model parameters of Tables II and III and are also relative to a value of 100 for the 624-keV 3^+ transition. The theoretical cross sections are summed values, from 3.8 to 73° c.m. The last column was obtained with a WS form factor.

with the inclusion of a factor of 3 enhancement in the $S=0$ transfer, the calculated 0^+ cross-section sum remains a factor of 5 weaker than the experimental one. Before attempting to explain this discrepancy in terms of a nuclear-structure effect, it may be worthwhile to examine some possible sources of uncertainty in the calculated cross sections. One might expect some problems when trying to compare states which differ widely in excitation energy, here by 7 MeV.

As mentioned previously, the DW calculations have been carried out with both a WS and an HO form factor. In the HO calculation, the form factor decays with a Hankel-function dependence, the asymptotic behavior of which is determined by the separation energy of the pair. In this method, the DW code searches for a matching radius where the slopes of the bound-state wave function and the decaying Hankel function are the same. This

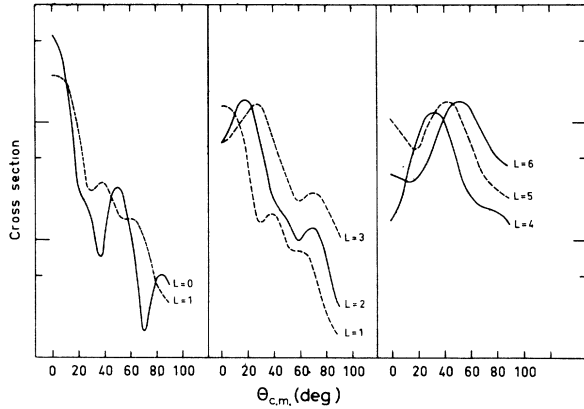


FIG. 8. Theoretical DWBA curves for odd- and even- L transfers in the reaction $^{46}\text{Ca}(^3\text{He}, p)^{48}\text{Sc}$. The AX optical-model potential has been used.

can introduce some uncertainty, depending on whether the tail matches at the same radius, independent of the excitation energy, or at slightly different radii. Any small differences in matching radii are compensated for by corresponding small changes in the value of the size parameter of the oscillator. This unphysical procedure can lead to appreciable variations in the calculated cross sections, particularly over wide ranges of excitation energy and in light nuclei.²⁶ However, we find that in the present analysis of the reaction $^{46}\text{Ca}(^3\text{He}, p)^{48}\text{Sc}$, the sensitivity of the calculated cross sections to the matching radius represents no more than a 30% effect for the 6.685-MeV transition, independent of the optical model employed in the DW calculations.

In the WS code, the calculated cross sections can be sensitive not only to small changes in the geometrical parameters of the WS well,²⁷ but also to the choice of binding energies. One may either choose binding energies for the individual nucleons corresponding to the appropriate single-particle energies²⁸ or corresponding to $\frac{1}{2}$ the separation energy of the pair. This latter procedure,

TABLE V. $^{46}\text{Ca}(^3\text{He}, p)^{48}\text{Sc}$ theoretical cross sections. The theoretical cross sections are again summed values and are given in the same units as in Table IV. The calculations are shown only for the AX optical potential.

E_x (keV)	J	$(f_{7/2})^{-1}f_{7/2}$	$(f_{7/2})^{-1}f_{5/2}$	$(f_{7/2})^{-1}p_{3/2}$	$(p_{3/2})^2$	$p_{1/2}p_{3/2}$
2085	5^+	125	85	1220		
2295	2^+	265	65	2020	1370	2700
2690	4^+	170	195	810		
3510	3^+	125	150	660	1900	
4175	1^+	185	460		1475	2200
5215	2^+	340	85	2550	1900	3450
5750	1^+	195	480		1545	2290
6250	3^+	160	185	830	2340	

for example, leads to a wide (nonphysical) variation in the depth of the WS well. We have examined these effects for the 6.685-MeV transition in the reaction $^{46}\text{Ca}(^3\text{He}, p)^{48}\text{Sc}$ and find that varying the binding energy of each nucleon by as much as $\pm 25\%$ results in a variation of the calculated cross section for the $T=4$, 0^+ transition of $\pm 30\%$ (see also Ref. 5).

Thus the WS and HO calculations for the 6.685-MeV transition give the same results to within 20 or 30%, consistent with the previous comparison shown in Table IV. Moreover, Bayman has recently shown²¹ that zero-range calculations of two-nucleon-transfer cross sections agree well in relative magnitude with the more complex finite-range calculations.

We have also checked the energy variation of the real well depth for the outgoing (proton) channel in the DW calculations, choosing an increase of 1 MeV per MeV increase of excitation energy. This is in the correct direction to compensate for the decreasing proton energy, although the magnitude of the change is surely excessive.^{16, 17} However, this again resulted in calculated cross sections for the analog-state transition which were within 20% of the values given in Table IV. Finally, we considered that the transferred pair in the $(^3\text{He}, p)$ $T=4$ transition should be bound as a neutron-neutron pair, i.e., the form factor should correspond to that for the $^{46}\text{Ca}(t, p)^{48}\text{Ca}$ ground-state transition. This makes a 7 MeV difference in the binding energy and also considerably worsens the agreement between calculation and experiment.

Consequently, we feel that the disagreement between the experimental and calculated $(f_{7/2})^{-1}f_{7/2}$ cross sections for the 0^+ analog state in ^{48}Sc is of order 5, and cannot be explained by any reasonable modification of the two-nucleon form factor and/or the optical-model parameters in the DW calculations.

It is clear from the theoretical comparison of Table V that any $2p$ contribution to the analog-state transition will lead to a large change over what is predicted on the basis of pure $(f_{7/2})^{-1}f_{7/2}$. In fact, there is already good evidence from the $^{46}\text{Ca}(t, p)^{48}\text{Ca}$ data on 0^+ states that such admixtures are required.^{29, 30}

The percentage amounts of $(2s-1d)^{-2}$ hole structure in the ^{46}Ca ground state and of $(2p)^2$ particle structure in the ^{48}Ca ground state are small, but even small admixtures can make an appreciable difference in the two-nucleon-transfer cross section to a single correlated state. Such admixtures are found to be of order 5% from single-nucleon stripping^{24, 25} and pickup data.³¹ An interpretation of these data³² has yielded the following form fac-

tor overlap for the ground-state reaction $^{46}\text{Ca}(t, p)^{48}\text{Ca}$:

$$0.94(1f_{7/2})^2 - 0.14(2s_{1/2})^2 - 0.19(1d_{3/2})^2 \\ + 0.22(2p_{3/2})^2 + 0.10(2p_{1/2})^2.$$

The phases are chosen to give a state which is constructively coherent. Such a form factor provides a basis for understanding the observed relative cross sections to the 0^+ states in the reaction $^{46}\text{Ca}(t, p)^{48}\text{Ca}$, as well as the absolute cross section³² for the ground-state transition. This overlap results in a factor of 5-6 increase in the calculated ground-state cross section over that expected for pure $(f_{7/2})^2$. This result may seem surprising when considering that the $2s-1d$ and $2p$ admixtures represent only 10% of the total probability, but it is a consequence of the very favorable $\lambda=0$ overlaps that these orbits provide in the two-nucleon-transfer reaction.^{12, 13, 21} Since the same overlap of course enters into the 6.685-MeV analog-state transition in the reaction $^{46}\text{Ca}(^3\text{He}, p)^{48}\text{Sc}$, the factor of 5-6 enhancement provides a very natural explanation for the discrepancy apparent in the $(f_{7/2})^{-1}f_{7/2}$ comparisons of Table IV. Indeed, such a factor brings the calculated cross sections into much better agreement with the experimental results.

The importance of including configuration mixing in order to reproduce the strength to the 0^+ member of the $(f_{7/2})^{-1}f_{7/2}$ multiplet, implies that similar mixing should also be considered for the other members. Mixing with the $2s$, $1d$, and $2p$ levels will mainly affect the low-spin states. If this mixing occurs with the right phases, then the calculated cross sections for these states would also be enhanced over the predictions of the pure $f_{7/2}$ model. On the other hand, the states of higher spin, particularly the 6^+ and 7^+ states, would presumably exhibit less configuration mixing, and thus their cross section should be closer to that predicted by the pure $f_{7/2}$ model. The previously noted final-state spin-dependent discrepancy (see Table IV) can then be qualitatively understood in terms of the above small admixtures. Such admixtures could not appreciably alter the one-nucleon-transfer spectroscopic factors for pure $f_{7/2}$ transfer,³ but might have some effect on the $(^3\text{He}, t)$ cross sections.² Let us finally reiterate that the above conclusions were made assuming that the DW codes can correctly predict the relative $(^3\text{He}, p)$ cross sections for a range of L values. Further experiments on the structure of the low-lying ^{48}Sc states are important for testing our main conclusions.

*Present address: Department of Chemistry, University of British Columbia, Vancouver 8, Canada

†Work supported in part by the Rask-Ørsted Foundation in Denmark.

‡Work supported in part by the U. S. Atomic Energy Commission.

§Work supported in part by the National Science Foundation.

¹J. J. Schwartz and B. A. Watson, *Phys. Letters* **29B**, 567 (1969); G. Bruge, A. Bussiere, H. Faraggi, P. Kossanyi-Demay, J. Loiseaux, R. Roussel, and L. Valentin, *Nucl. Phys.* **A129**, 417 (1969).

²H. Ohnuma, J. Erskine, J. Schiffer, J. Nolen, and N. Williams, *Phys. Rev. C* **1**, 496 (1970), and references contained therein.

³J. L. Yntema and G. R. Satchler, *Phys. Rev.* **134B**, 976 (1964); J. J. Schwartz, *Phys. Rev. Letters* **18**, 174 (1967); H. Ohnuma and J. L. Yntema, *Phys. Rev. C* **2**, 1725 (1970).

⁴K. Grotowski, S. Wiktor, and F. Pellegrini, *Nuovo Cimento* **47B**, 255 (1967); R. A. Wallen, H. Ohnuma, and N. Hintz, *Bull. Am. Phys. Soc.* **14**, 601 (1969).

⁵D. G. Fleming, R. Broglia, K. Abdo, O. Nathan, D. Pullen, B. Rosner, and O. Hansen, preceding paper, *Phys. Rev. C* **5**, 1356 (1972).

⁶J. H. Bjerregaard, O. Hansen, and G. Sidenius, *Phys. Rev.* **138**, 1097 (1965).

⁷J. A. Nolen, J. Schiffer, N. Williams, and D. von Ehrenstein, *Phys. Letters* **18**, 1140 (1967); F. D. Bechetti, D. Dehnard, and T. G. Dzubay, *Nucl. Phys.* **A168**, 151 (1971).

⁸H. Ohnuma, J. Erskine, J. Nolen, J. Schiffer, and P. Roos, *Phys. Rev.* **177**, 1695 (1969); C. Moazed, K. Nagatani, and A. Bernstein, *Nucl. Phys.* **A139**, 1 (1969); J. Laget, J. Vervier, G. Bruge, J. Loiseaux, and L. Valentin, *ibid.* **A125**, 481 (1969).

⁹W. Schlegel, D. Schmitt, R. Santo, and F. Pühlhofer, *Nucl. Phys.* **A153**, 502 (1970).

¹⁰C. Chasman, K. Jones, and R. Ristinen, *Phys. Rev.* **140B**, 212 (1965).

¹¹D. G. Fleming, to be published.

¹²B. F. Bayman and A. Kallio, *Phys. Rev.* **156**, 1121 (1967).

¹³N. K. Glendenning, *Phys. Rev.* **137B**, 102 (1965); R. A. Broglia and C. Riedel, *Nucl. Phys.* **A92**, 145 (1967); **A93**, 241 (1967).

¹⁴E. R. Flynn, D. Armstrong, J. Beery, and A. Blair, *Phys. Rev.* **182**, 1113 (1969).

¹⁵N. Nakashina, Y. Chiba, Y. Awaya, and K. Matsuda,

Nucl. Phys. **A140**, 417 (1970).

¹⁶F. G. Perey, *Phys. Rev.* **131**, 745 (1963).

¹⁷F. D. Bechetti and G. W. Greenlees, *Phys. Rev.* **182**, 1190 (1969).

¹⁸J. C. Hardy and I. Towner, *Phys. Letters* **25B**, 98 (1967).

¹⁹D. G. Fleming, J. Cerny, and N. Glendenning, *Phys. Rev.* **165**, 1153 (1968); D. G. Fleming, J. Hardy, and J. Cerny, *Nucl. Phys.* **A162**, 225 (1971).

²⁰J. M. Nelson, N. Chant, and P. Fisher, *Nucl. Phys.* **A156**, 406 (1970).

²¹B. F. Bayman, *Phys. Rev. Letters* **25**, 1768 (1970).

²²W. R. McMurray, M. Peisach, R. Pretorias, P. van der Merwe, and I. van Heerden, *Nucl. Phys.* **A99**, 6 (1967); W. J. McDonald, J. Sample, D. Sheppard, G. Stinson, and K. Jones, *Phys. Rev.* **171**, 1254 (1968).

²³T. A. Belote, F. Tak Dao, W. Dorenbusch, J. Kuperus, and J. Rapaport, *Phys. Letters* **23**, 480 (1966); L. Meyer-Schützmeister, D. Gemmel, R. Holland, F. Kuchnir, H. Ohnuma, and N. Puttaswami, *Phys. Rev.* **187**, 1210 (1969); W. G. Davies, J. Hardy, and W. Darcy, *Nucl. Phys.* **A128**, 465 (1969); A. Graue, J. Lien, L. Rasmussen, F. Sandvik, and E. Cosman, *ibid.* **A162**, 593 (1971); J. D. Garrett, R. Middleton, D. Pullen, S. Andersen, O. Nathan, and O. Hansen, *ibid.* **A164**, 449 (1971).

²⁴E. Kashy, A. Sperduto, H. Enge, and W. Buechner, *Phys. Rev.* **135B**, 865 (1964); J. R. Erskine, A. Marinov, and J. Schiffer, *ibid.* **142**, 633 (1966).

²⁵T. A. Belote, H. Chen, O. Hansen, and J. Rapaport, *Phys. Rev.* **142**, 624 (1966); J. J. Schwartz, J. Alford, and A. Marinov, *ibid.* **153**, 1248 (1966).

²⁶D. G. Fleming, J. Cerny, C. Maples, and N. Glendenning, *Phys. Rev.* **166**, 1012 (1968).

²⁷S. M. Smith and A. Bernstein, *Nucl. Phys.* **A125**, 339 (1969).

²⁸R. L. Jaffe and W. J. Gerace, *Nucl. Phys.* **A125**, 1 (1969); D. G. Fleming and B. Sørensen, to be published.

²⁹J. H. Bjerregaard, O. Hansen, O. Nathan, R. Chapman, S. Hinds, and R. Middleton, *Nucl. Phys.* **A103**, 33 (1967).

³⁰B. F. Bayman and N. M. Hintz, *Phys. Rev.* **172**, 1113 (1968); P. Federman and S. Pittel, *Nucl. Phys.* **A155**, 161 (1970).

³¹T. W. Conlon, B. Bayman, and E. Kashy, *Phys. Rev.* **144**, 941 (1966); R. J. Petersen, *ibid.* **170**, 1003 (1968); D. Schmitt and R. Santo, *Z. Physik* **233**, 114 (1970).

³²E. R. Flynn and O. Hansen, *Phys. Letters* **31B**, 135 (1970).